

## AN EXAMINATION ON OBSERVED RESULTS OF GROUND STRAINS DURING EARTHQUAKES

S.MORICHI\*, Y.IMAMURA\*, M.SAEKI\*\*, T.TAKANO\* and K.ODA\*

\* Department of Civil Engineering, Faculty of Industrial Science  
and Technology, Science University of Tokyo, 2641 Yamazaki, Noda-shi  
Chiba, 278, Japan

\*\* Japan Engineering Consultants Co.Ltd.  
5-33-11, Honcho, Nakano-ku, Tokyo, 164, Japan

### ABSTRACT

It is fundamental to examine engineering properties of earthquake induced ground strains for studying seismic resistance of underground structures. In this paper, direct measurement system of ground strains were devised and observed results were analysed. Three normal strains on surface of ground were observed and analysed for purpose of inspecting properties of strain conditions. More than 100 earthquake records were obtained and they were found to be on nearly pure shear condition. The gauge length of this device is 1m, which seems to be too short from viewpoint of earthquake engineering. Under such consideration, same typed measurement system was installed on observation site apart 16m from the above mentioned one, for the purpose of inspecting strain condition in the wide-spread area. Examining the results obtained on two sites, it was revealed that pure shear condition were produced.

### KEYWORDS

Earthquake observation, Earthquake induced ground strain, Ground strain condition

### INTRODUCTION

Examination on earthquake resistance of underground structure became to be important increasingly, taking account of the heavy damage of subway tunnel due to the 1995 Southern Hyogo Prefecture earthquake. Underground structure is forced to be moved with the surrounding soil and it does not move freely as a structure on the ground surface. Therefore, seismic behavior and general characteristics of ground strain are essential parameter for seismic design of these structures.

Various studies have been conducted to observe strains on underground structures during earthquakes. Ground strain is considered to be almost equal to observed one (Sakurai *et al*, 1967) (Tamura *et al*, 1975) (Sato *et al*, 1986). Another approach to estimate ground strains bases on the strong ground motion record. Ground motion data at only one or a few accelerographs were able to be incorporate into analyses (Kamiyama, 1976) (Takada *et al*, 1980). The recent development of closely spaced arrays is available for estimating ground strains (Noda *et al*, 1988) (Katayama *et al*, 1990) (Arakawa *et al*, 1984). A

time-space stochastic process model is used for estimation of ground strains(Tamura *et al*,1992).

Undirect measurements of ground strain were utilized in the studies mentioned above. In order to obtain data of ground strain with higher accuracy,direct measurement is desired to be devised. Considering this background,the object of this paper is laid on the development of direct measurement method for ground strain and also investigation on the observed results.

## OBSERVATION METHOD

### Observation Site

The observation site is located in the campus of the Science University of Tokyo(Noda city,Chiba). It is situated in lat.35° 55' 03" N and log.139° 54' 57" E. The topographical condition of the site is generally simple with the ground surface being almost flat. Typical soil properties obtained from representative borehole is shown in Fig.1. The site consists of ground with silt stratum more than 30m thick in which there are sandy layers.

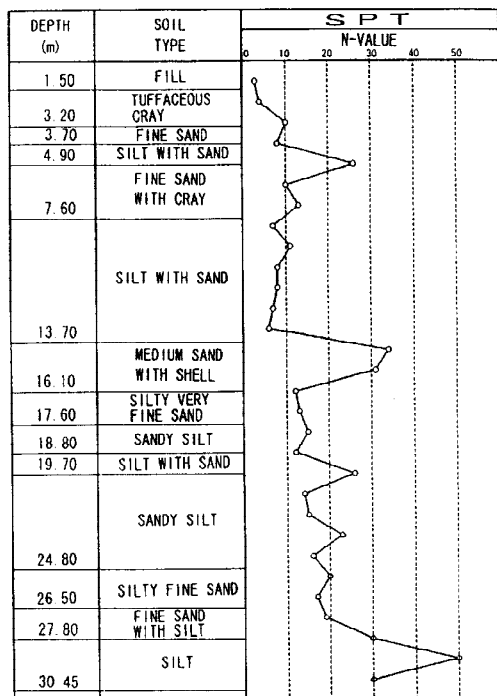


Fig.1 The result of SPT at the site

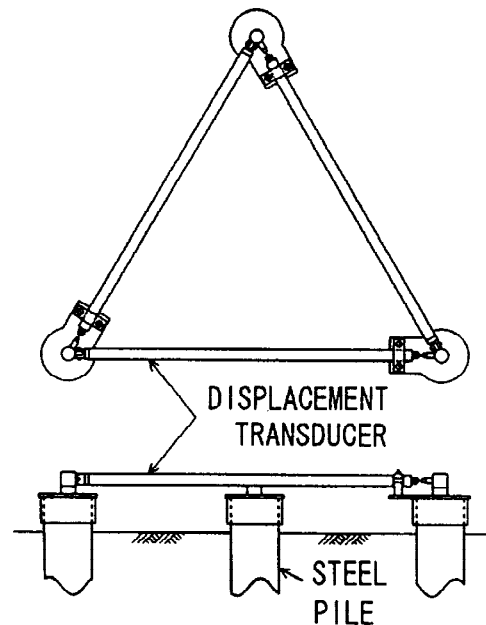


Fig.2 The schematic layout of measurement apparatus

### Observation Method

The observation began in 1988. Three components of normal strain produced on ground surface were observed. Steel piles(Outer diameter:75mm,Thickness:4mm) were driven on three points which correspond to vertices of a triangle with sides having 1m in length. Driving depth was about 70 cm. Earthquake-induced relative displacements between piles were directly observed by use of displacement transducers(DS-100:Tokyo Sokushin Co.Ltd,Weight:2.1kg). The observed results were divided by original length(1m),in order to calculate strains.

Distance between piles corresponds to gauge length, which is one of the most important elements to be considered for strain measurement. It must be determined by taking account of various factors. In this paper, gauge length is determined only from practical viewpoint such as maintenance of the apparatus, mechanical restriction of transducer and so on. Figure 2 shows the schematic layout of measurement apparatus. For purpose of inspecting properties of ground strains in the wide-spread area, same typed equipment was situated on the other site apart 16m from the site mentioned above. Observation on both sites began on June 2nd 1994.

Furthermore, in the observation site, three components piezo-electric accelerometers (PV-22: Rion Co. Ltd) were installed. Triggering of the signals is performed when ground acceleration exceeds a present threshold level (in this paper 1.0 gal). The signals from transducers are transmitted to the observation room, where they are automatically digitalized with the sampling interval of 1/100sec by A/D converter. The recorder has a digital magnetic tape with a recording capacity of more than 1 hour. Timing information is internally generated, in addition, the absolute time is corrected hourly by utilizing the signal from N.H.K. (The Japan Broadcasting Corporation).

A general layout of seismometers as well as measuring device for strains is shown in Fig. 3. A1, A2 and A3 indicate the locations of accelerometers. Accelerometers installed in A1 and A2 were damaged a few years after beginning of observation, and one situated on A3 also was spoiled on June 2nd 1994. In this paper, data from A3 indicate as acceleration of the site. After July 1994, servo-accelerometer (PCS-1025: Tokyo Sokushin Co. Ltd) was installed on A4. This is used for measuring acceleration and triggering. Strain-1 means measuring site of ground strain used from beginning of observation and Strain-2 is one situated later.

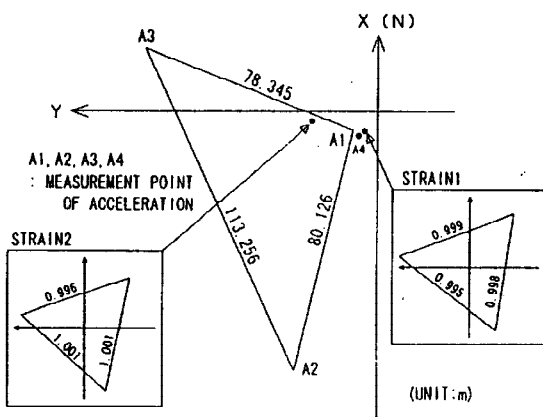


Fig. 3 Layout of the observation site

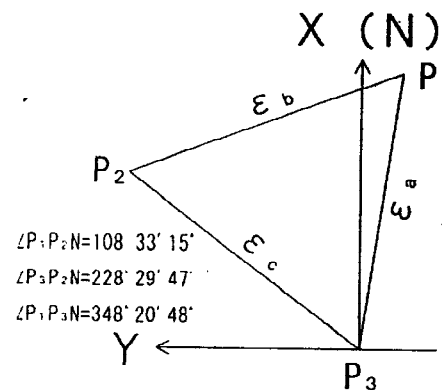


Fig. 4 The coordinate system of Strain-1

## EXAMINATION ON OBSERVED RESULTS

### Results observed in the site Strain-1

A total of 119 earthquakes have been recorded. By using observation records of ground strains, two components of normal strains ( $\epsilon_x$ ,  $\epsilon_y$ ) and shear strain ( $\gamma_{xy}$ ) were calculated for inspecting properties of strains (As indicated in Fig. 4, direction of x-axis is corresponded to north). Figure 5 shows ground strains ( $\epsilon_x$ ,  $\epsilon_y$ ,  $\gamma_{xy}$ ) of the observation result which was recorded on March 23 1995. Inspecting the results, phase angle between  $\epsilon_x$  and  $\epsilon_y$  seems almost  $\pi$ . Figure 6 shows time history of principal strains ( $\epsilon_1$ ,  $\epsilon_2$ ), max. shear strain ( $\gamma_{max}$ ) and angle  $\theta$  between direction of max. principal strain and x-axis. It is found that variation of  $\theta$  is about  $90^\circ$ .

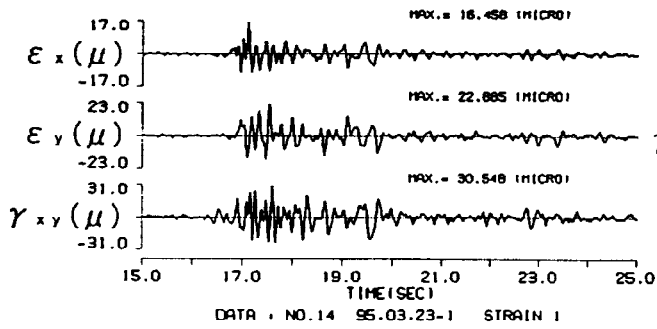


Fig.5 The time variation of  $\epsilon_x, \epsilon_y, \gamma_{xy}$

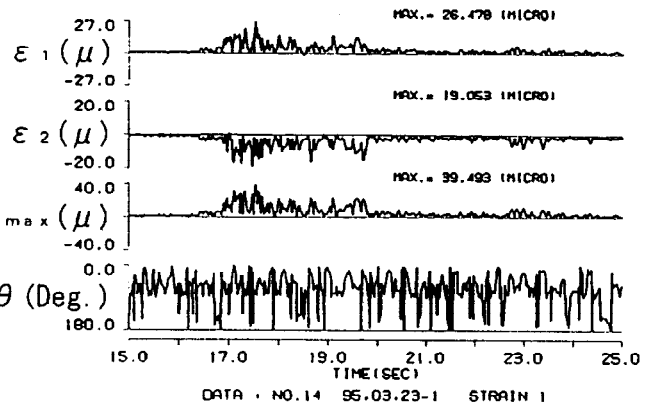


Fig.6 The time variation of  $\epsilon_1, \epsilon_2, \gamma_{max}$  and  $\theta$

Variation in every 1/100 second of Mohr strain circle were demonstrated in Fig.7. Coordinates of small black circle means  $(\epsilon_x, \gamma_{xy}/2)$ . Investigating the results, the followings are obtained.

- ① When radius of Mohr circle shows minimum value,  $\theta$  changes almost by  $90^\circ$  suddenly. On the other hand,  $\theta$  is almost constant, when radius shows large value.
- ② During radius shows large value, Mohr circle contains original point of  $(\epsilon, \gamma/2)$  plane.

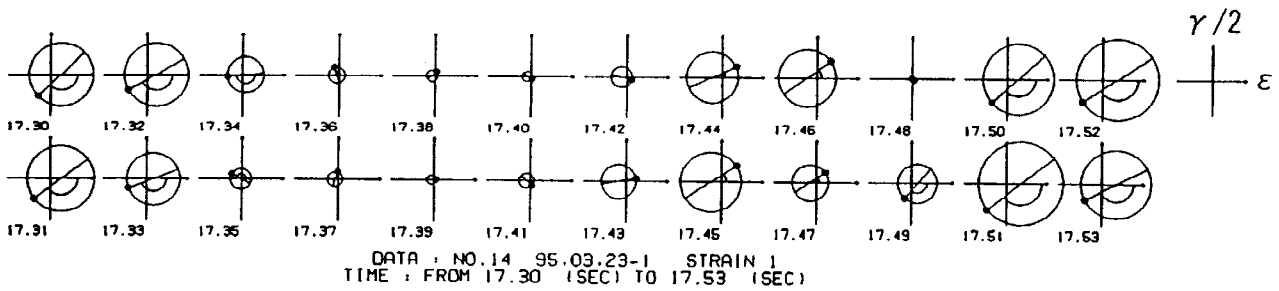


Fig.7 The variation of Mohr's strain circle

The above were investigated deeply in the following. Concerning ①, probability density of  $\theta$  between maximum principal strain and x-axis were calculated. An example is shown in Fig.8. Two peaks were found easily in probability density and difference of them is about  $90^\circ$ . As for all records, number of earthquakes is shown in abscissa and values of two peaks of  $\theta$  were plotted on ordinate as shown in Fig.9. At a glance, direction of maximum principal strain is almost constant for all earthquakes.

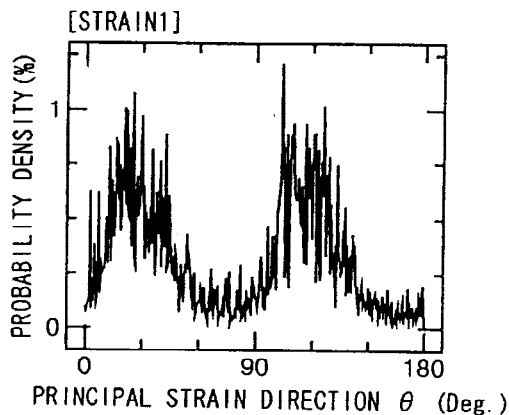


Fig.8 Probability density distribution of principal strain direction

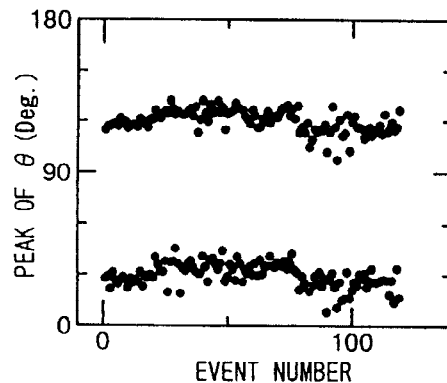


Fig.9 Relation between the peak of  $\theta$  and the event number

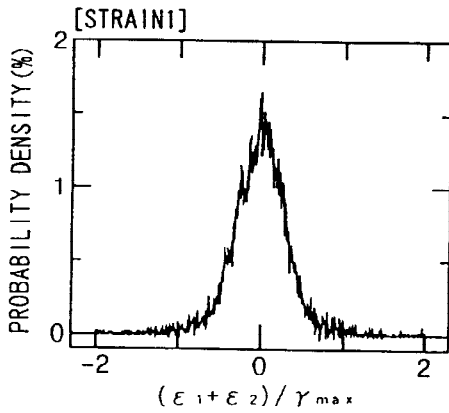


Fig.10 Probability density distribution of the ratio  $(\epsilon_1 + \epsilon_2) / \gamma_{max}$

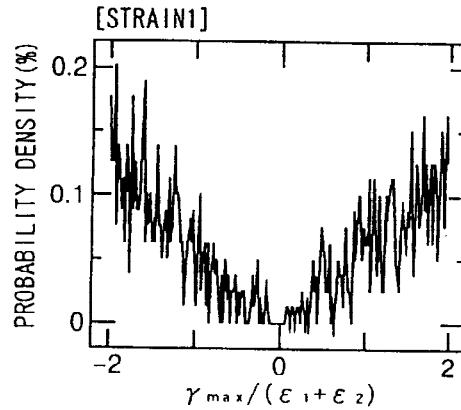


Fig.11 Probability density distribution of the ratio  $\gamma_{max} / (\epsilon_1 + \epsilon_2)$

Concerning②, probability density of sum of principal strains ( $\epsilon_1 + \epsilon_2$ ) divided by max. shear strain  $\gamma_{max}$ ,  $((\epsilon_1 + \epsilon_2) / \gamma_{max})$  during duration time are shown in Fig.10. Curve of probability density seems to have the peak at 0 which means pure shear state. In order to inspect the probability in which  $\epsilon_1 = \epsilon_2$ , value of  $(\gamma_{max} / (\epsilon_1 + \epsilon_2))$  were calculated as shown in Fig.11. States which show pure dilatation condition were not able to find. In case of pure shear state, center of Mohr circle corresponds to the original point. The strain state shown in this case seems nearly pure shear condition. All other records have the same characteristics to this case.

Event number of earthquakes, maximum value of  $\gamma_{max}$  more than  $3.5 \mu$ , maximum absolute values of principal strains ( $\epsilon_1$  or  $\epsilon_2$ ) and maximum value of acceleration in time history were listed in Table-1. Acceleration means resultant component calculating from two horizontal and vertical component.

Table1 The list of observation records

No.	Date	Time	Epicenter		Hypocenter			Maximum Value		
			Region	Dis. (km)	Latitude Longitude	Depth (km)	M, *	ACCEL. (gal)	STRAIN ( $\mu$ )**	$\epsilon$
1	89.02.19	21:27:18	SOUTH WESTERN IBARAGI PREF.	11	36° 01.1' N 139° 54.5' E	55	5.6	83.5	13.4	24.9
2	90.08.05	12:36:59	EAST OFF IBARAGI PREF.	120	36° 24.1' N 141° 06.6' E	39	5.8	6.26	2.10	3.73
3	90.08.23	08:47:31	KUJUKURI COAST BOSO PENINSULA	77	35° 20.7' N 140° 23.8' E	50	5.4	6.96	2.68	4.21
4	90.10.06	23:33:26	SOUTH WESTERN IBARAGI PREF.	89	36° 29.1' N 140° 36.8' E	51	5.0	13.3	2.86	4.39
5	91.10.19	08:31:26	SOUTH WESTERN IBARAGI PREF.	18	36° 05.0' N 139° 55.2' E	59	4.3	19.1	2.21	3.86
6	91.11.19	17:24:16	MIDDLE CHIBA PREF.	36	35° 36.3' N 140° 01.5' E	81	4.9	14.7	1.87	3.59
7	93.05.21	11:36:46	SOUTH WESTERN IBARAGI PREF.	14	36° 02.5' N 139° 54.0' E	61	5.3	141.	21.9	40.6
8	93.10.12	00:55:40	FAR SOUTH OFF TOKAI	459	32° 01.3' N 138° 14.4' E	390	7.1	18.9	7.70	12.6
9	94.10.04	22:25:40	EAST OFF HOKKAIDO	1060	44° 22' N 147° 40' E	30	8.1	15.3	3.95	6.47
10	94.11.04	19:06:36	SOUTH WESTERN IBARAGI PREF.	17	36° 04' N 139° 55' E	59	4.5	35.5	4.18	7.07
11	94.12.28	21:22:12	FAR OFF SANRIKU	603	40° 27' N 143° 43' E	0	7.5	5.23	3.16	5.99
12	95.01.07	07:39:53	IWATE PREF.	533	40° 3' N 142.4' E	30	6.9	5.31	2.02	3.96
13	95.01.07	21:34:52	SOUTH WESTERN IBARAGI PREF.	41	36° 17' N 139° 59' E	70	5.4	60.9	8.50	12.4
14	95.03.23	07:24:41	SOUTH WESTERN IBARAGI PREF.	22	36° 06' N 140° 01' E	58	5.1	131.	6.24	11.5
									26.5	39.5
									13.6	24.4

\*1 Magnitude by Japan Meteorological Agency  
\*2 upper STRAIN1, lower STRAIN2

Inspecting values of strain listed in the Table-1 for each earthquakes, maximum value of  $\gamma_{max}$  is almost twice of one of principal strain. In Fig.12, relation between maximum value of  $\gamma_{max}$  and one of absolute values of principal strains is shown for all observation records up to now. This relation is formulated as follows(1) and endorses that pure shear state produced.

$$\gamma_{max} = 1.74 \times \max(|\epsilon_1|, |\epsilon_2|)^{0.97}$$

[STRAIN-1] (1)

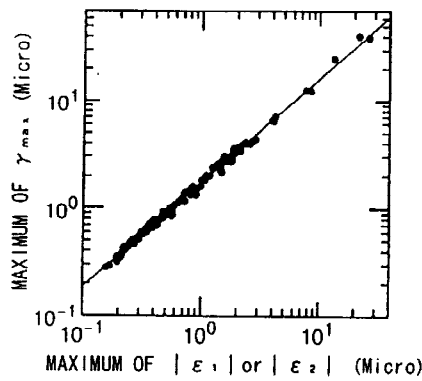


Fig.12 Relation between the max of  $\gamma_{max}$  and the max.of  $|\epsilon_1|$  or  $|\epsilon_2|$

Figure.13(14) shows relation between maximum value of maximum shear strain(absolute value of maximum principal strain) and maximum value of acceleration. Two figures show that strain is thought to be increased with increase of acceleration. Furthermore, maximum strain corresponding to a given acceleration increases with seismic magnitude.

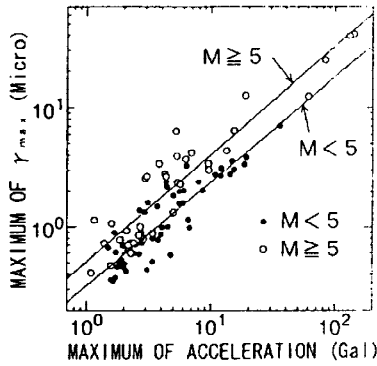


Fig.13 Relation between the max.of  $\gamma_{max}$  and the max.of acceleration

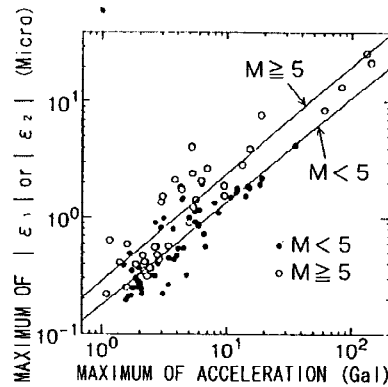


Fig.14 Relation between the max.of  $|\epsilon_1|$  or  $|\epsilon_2|$  and the max.of acceleration

Figure 15(16) shows relation between maximum value of maximum shear strain(absolute value of maximum principal strain) and epicentral distance. Value of strain corresponding to a given epicentral distance increases with seismic magnitude. Furthermore,attenuation of maximum strain seems to become gentle with increase in seismic magnitude. Similar indications(Nakamura *et al*,1982),(Okamoto,1984) were reported.

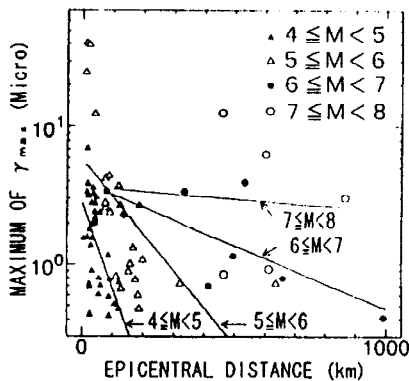


Fig.15 Relation between the max.of  $\gamma_{max}$  and Epicentral distance

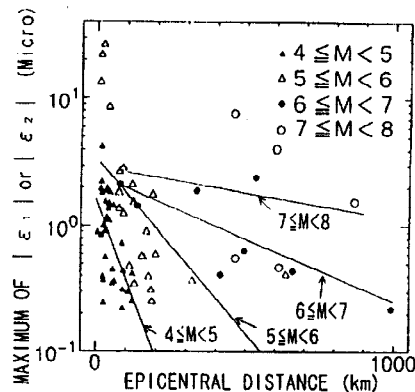


Fig.16 Relation between the max.of  $|\epsilon_1|$  or  $|\epsilon_2|$  and Epicentral distance

Comparison between records(Strain-1) and ones(Strain-2)

Same typed system(Strain-2) was installed and began earthquake observation on June 1994. Mohr strain circle calculated with a record observed in both sites were shown in Fig.17. As a whole,they don't seem to be similar each other. In the followings,properties of both data were examined.

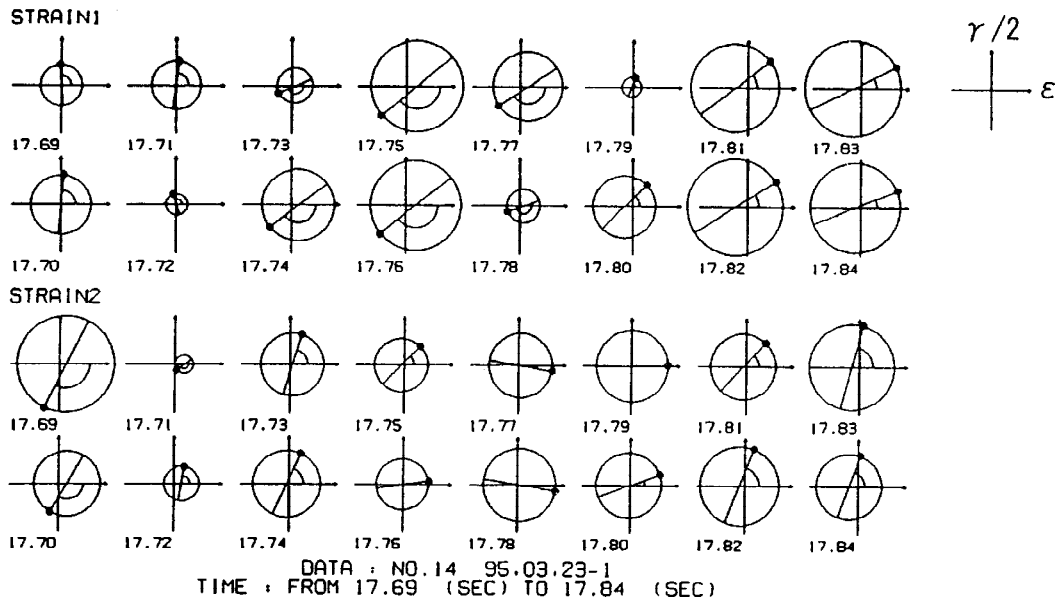


Fig.17 Comparison of Mohr's strain circle of strain-1 and strain-2

In the similar way as Fig.8 and Fig.9,probability density of angle  $\theta$  was calculated and obtained two peaks were plotted as shown in Fig.18. White circles were obtained for strain-2,and directions of maximum principal strains seems to same as the case for Strain-1. Also,in the same manner as Fig.10,probability density of  $((\epsilon_1 + \epsilon_2) / \gamma_{max})$  were calculated and the result is shown in Fig.19. At a glance,this is similar to the one of strain-1.

Relation between maximum values of  $\gamma_{max}$  and one of absolute values of principal strains are calculated for all observation records of strain-2. The follow is the result.

$$\gamma_{max} = 1.88 \times \max(|\epsilon_1|, |\epsilon_2|)^{1.01} \quad \text{[STRAIN-2]} \quad (2)$$

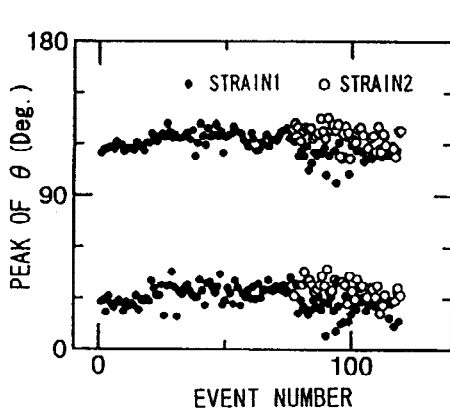


Fig.18 Relation between the peak of  $\theta$  and the event number

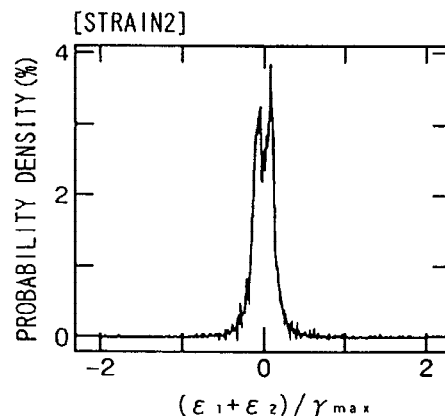


Fig.19 Probability density distribution of principal strain direction

As shown in the above, strain conditions on both sites seem to be quite similar.

## CONCLUSIONS

Strains produced on the ground surface were observed during earthquakes and properties of strain condition were investigated. Gauge length is 1m, which seems to be too short from earthquake engineering point of view. Then, same typed apparatus is installed in new site, and began observation in two sites. Examining the results, the followings were obtained.

- ① Almost pure shear strain conditions were produced in the spread area.
- ② Directions of principal strains are almost same for all observation results.
- ③ Maximum values of maximum shear strains are nearly twice to ones of absolute principal strain during duration time of records
- ④ Strain is thought to be increased with increase of acceleration. Maximum strain corresponding to a given acceleration increases with seismic magnitude.
- ⑤ Strain value corresponding to a given epicentral distance increases with seismic magnitude. Attenuation of maximum strain seems to become gentle with increase in seismic magnitude.

## REFERENCES

- Sakurai, A., Takahashi, T., Tsutsumi, H., Yajima, H., Noguchi, T. and Iwakata, T. (1967). Dynamic Stresses of Underground Pipe Lines during Earthquakes, *Report of Research Laboratory*, Central Research Institute of Electric Power Industry, **67058**
- Tamura, C., Okamoto, S. and Hamada, M. (1975). Dynamic Behavior of a Submerged Tunnel during Earthquakes, *Report of the Institute of Industrial Science*, the University of Tokyo, Vol.24, No.5.
- Sato, N., Nakamura, M., Iwamoto, T. and Ohbo, N. (1986). Observation of Seismic Ground Motion and Buried Pipe Strain, *Proc. of 7th Japan Earthquake Engineering Symposium*. 583-588.
- Kamiyama, M. (1976). Stress and Strain in Ground during Earthquake, *Proc. of Japan Society of Civil Engineers*, **250**. 9-24.
- Takada, K. and Wright, J.P. (1980). Earthquake Relative Motions for Lifelines, *Proc. of Japan Society of Civil Engineers*, **299**. 13-20.
- Noda, S., Kurata, E. and Tsuchida, H. (1988). Observation of Earthquake Motions by Dense Instrument Arrays at Soft Ground, *Proc. of 9th World Conference on Earthquake Engineering*, 221-226.
- Katayama, T., Yamazaki, K., Nagata, S., Lu, L. and Turker, T. (1990). Development of Strong Motion Data Base for the Chiba Seismometer Array, *Report of Earthquake Disaster Mitigation Engineering Laboratory*, **14**, Institute of Industrial Science, University of Tokyo.
- Arakawa, T., Kawashima, K., Tamura, K., Aizawa, K. and Takahashi, K. (1984). Dense Instrument Array Observation by Public Works Research Institute - Observation System at Numazu Site -, *Technical Memorandum of PWRI*, **2140**
- Tamura, K. and Aizawa, K. (1992). Differential Ground Motion Estimation Using a Time-Space Stochastic Process Model, *Proc. of Japan Society of Civil Engineers*, **441/1**. 18.49-56.
- Nakamura, M., Katayama, T. and Kubo, K. (1982). Quantitative Study on Observed Seismic Strains in Underground Structures, *Proc. of Japan Society of Civil Engineers*, **320**, 35-46.
- Okamoto, S. (1984). Introduction to Earthquake engineering, University of Tokyo Press, ISBN4-13-068104(UPT 69042), ISBN 0-86008-361-6.